Numerical and Experimental Investigation of Aspect Ratio Effect on Aerodynamic Performance of NACA 4415 Airfoil Section at Low Reynolds Number

Hatice Cansu Ayaz Ümütlü[1] ✉ – Zeki Kıral[2] – Ziya Haktan Karadeniz[3]

1 Dokuz Eylul University, The Graduate School of Natural and Applied Sciences, Turkey
2 Dokuz Eylul University, Faculty of Engineering, Turkey
3 Izmir Institute of Technology, Department of Energy Systems Engineering, Turkey

✉ cansu.ayaz@deu.edu.tr

Abstract *In this study, the effect of aspect ratio on the aerodynamic coefficients is investigated for a NACA 4415 airfoil profile. Four different aspect ratios which are 3, 5, 7, and 9 are evaluated with the computational fluid dynamics (CFD) simulations and the experiments. The CFD studies are performed using a three-dimensional (3D) computational domain and by using the k–ω shear stress transport (SST) turbulence model for turbulence calculations. The measurements of the aerodynamic forces are carried out in open jet type wind tunnel using a three-component balance. CFD and experimental studies are performed at angles of attack from 0° to 25° and Reynolds number $85 \cdot 10^3$. The results show that as the aspect ratio increases, separation points move towards the leading edge of the airfoil and the stall angle reduces. Furthermore, it is observed that the lift coefficients increase with the increasing aspect ratio. The results obtained indicate that there is a harmony between the experimental data and the CFD solutions.*

Keywords *airfoil, wind tunnel, aspect ratio effect, aerodynamic coefficients, three-component balance, low Reynolds number*

Highlights:
▪ *The research investigates the aspect ratio effect on NACA 4415 airfoil at low Reynolds number.*
▪ *Four different aspect ratios are investigated both experimentally and numerically.*
▪ *Experiments and numerical studies show that with increasing aspect ratio, the coefficients of lift increase.*
▪ *The research demonstrates that with increasing aspect ratio, the stall angle reduces.*

1 INTRODUCTION

Airfoils are important components of many scientific and technological fields, including wind energy, aerospace, defense, transportation, jet engines, unmanned aerial vehicles (UAVs), mixing of fluid products, etc. [1] to [3]. There are many studies in the literature on the design and analysis of airfoil structures due to their frequency of use and importance in different industrial application areas. In aerodynamics, Reynolds numbers below $500 \cdot 10^3$ are typically considered to be in the low Reynolds number range. Generally, high Reynolds number studies are conducted and there is limited research in literature related to low Reynolds numbers. Winslow et al. [4] studied aerodynamic characteristics and separation characteristics at Reynolds numbers from $10 \cdot 10^4$ to $10 \cdot 10^5$. Akbiyik et al. [5] studied the aerodynamic performance of a NACA 0015 airfoil at a Reynolds number of $48 \cdot 10^3$ under different configurations of plasma actuator electrodes. Bartl et al. [6] investigated the lift, drag and surface pressure of an airfoil at low to moderate Reynolds numbers ranging from $50 \cdot 10^3$ to $600 \cdot 10^3$. Traub and Coffman [7] studied the leading and trailing edge flaps at Reynolds numbers of $40 \cdot 10^3$, $60 \cdot 10^3$, and $80 \cdot 10^3$. Their results showed that the flaps affect the aerodynamic characteristics positively. Xia et al. [8] briefed the flow structures of airfoils at low Reynolds numbers. They examined the laminar separation bubbles and their effects. Murayama et al. [9] studied the aerodynamic performances of the low Reynolds numbers airfoil to observe the effect of the robustness, and they used a flexible flap, a bird-inspired wing, in their experimental study. Ayaz Ümütlü et al. [10] experimentally revealed that the maximum lift and stall angle

at low Reynolds number condition are lower in comparison with the high Reynolds number region. Stutz et al. [11] investigated vertical gust and airfoil interaction at Reynolds numbers $12 \cdot 10^3$ and $54.4 \cdot 10^3$. Somashekar and Immanuel Selwynraj [12] examined the effect of rain on the aerodynamic characteristics of an airfoil operating at a Reynolds number of $200 \cdot 10^3$.

It is important to define the flow characteristic of the airfoil in order to improve the aerodynamic performance. The aspect ratio (AR) has a substantial impact on the aerodynamic behavior of the airfoil. In literature, there are studies considering the different aspects of the aspect ratio effects. Ananda et al. [13] studied on flat-plate wings with the aspect ratio range of 2 to 5 at low Reynolds numbers. They found that from the wind tunnel tests the Oswald's efficiency factors exhibited considerable sensitivity in aspect ratio changes. As the aspect ratio increased, it was observed that Oswald's efficiency factor declined. Lee et al. [14] numerically studied aspect ratio effects on a revolving wing. They used a rectangular wing and considered the Rossby number while conducting the study. The aspect ratio ranges of their study are 1 to 10. Awasthi et al. [15] experimentally studied the flow structure of the airfoil with the aspect ratio of 0.5. They presented that in an airfoil with such a low AR, the interactions of already existing complex flow structures are present even in the mid-span of the airfoil. Zanforlin and Deluca [16] studied the effects of the tip losses on the aspect ratio of the vertical axis wind turbines. They investigated the AR interval of 0.25 to 3. They performed three dimensional CFD analysis. They assessed high AR with low tip losses or low AR with higher losses airfoil to achieve the maximum power output. They identified the optimal aspect ratio that gives the highest

power. Lee and Han [17] studied NACA 0012 airfoil with the aspect ratios of 3, 4, 5, and 6 at high angle of attack (AoA). They measured lift and drag by load cells. Ayaz Ümütlü et al. [18] experimentally studied on NACA 4415 airfoil which has an aspect ratio of 9 and proposed a new approach for stall detection.

The NACA 4415 airfoil profile is a type of cambered airfoil that can be used in vertical-axis wind turbines (VAWTs). However, a few experimental studies are using NACA 4415 airfoil at low Reynolds number conditions. We aimed to fulfill this gap in the literature by investigating the NACA 4415 airfoil experimentally at Reynolds number 85·10³. Asr et al. [19] studied the start-up characteristics of H-Darrieus vertical-axis wind turbines using NACA airfoils. They utilized Ansys Fluent to conduct transient CFD analysis to investigate this behavior. Parker et al. [20] studied the effect of chord-to-diameter ratio on the wake of VAWTs. They investigated three different D/c ratios which are 3, 6, and 9 and they used NACA 0022 symmetrical airfoil in their experiments. Zhong et al. [21] studied the dynamic stall control using a leading-edge rod on the Darrieus vertical-axis wind turbine. They used NACA 4-digit symmetrical airfoil profiles in their study. Song et al. [22] studied on aerodynamic characteristics of the Darrieus vertical-axis wind turbine and they investigated varying thickness (12 %, 15 %, 18 %, and 21 %) of the airfoil using CFD simulations.

There are two important research which show the effects of the Reynolds number and the aspect ratio. Miley [23] published a catalog on the Reynolds number effect over the various airfoil profiles at different test conditions. It is seen from Fig. 1 that as the Reynolds number increases, the lift coefficient also increases. However, the aspect ratio is not detailly presented in Miley's study. Moreover, Ostowari and Naik [24] studied on the aspect ratio effect of the NACA 4415 airfoil at Reynolds number of 250·10³ for the aspect ratios of 6, 9, 12, and infinite span. Compared to Ostowari and Naik's [24] study, a lower Reynolds number is used in this paper while the aspect ratios are 3, 5, 7, and 9. The results of this paper are evaluated in the light of these two important studies in the literature. Fig. 1 shows some of the results of Miley's [23], and Ostowari and Naik's [24] studies. The main contribution of this paper is the investigation of the aspect ratio interval of the NACA 4415 airfoil under the low Reynolds number condition to cover the gaps that remained in the studies mentioned above.
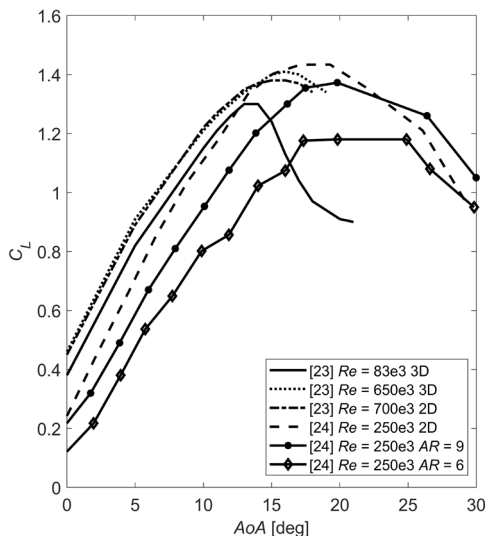
Fig. 1. The results of the studies of Miley [23], and Ostowari and Naik [24]

There are many studies on airfoils, but the number of studies considering the aspect ratio of the airfoil at low Reynolds number are limited. In the present study, NACA 4415 airfoil is selected as a model, and wind tunnel tests are conducted for four different aspect ratios of 3, 5, 7, and 9 at low Reynolds number conditions. Furthermore, the flow analyses are performed to compare the results. The objective of this paper is to determine the aspect ratio effect on the lift and drag coefficients of NACA 4415 airfoil section. In addition, since it is difficult to study at low Reynolds numbers, we aimed to fill the experimental study gap in the literature with this study by examining the aspect ratio at 85·10³ Reynolds number. For obtaining the lift and drag coefficients, a three-component balance system is utilized in the experiments.

This paper is structured as follows: The methods and materials section explains the numerical and experimental procedures. In the results and discussions section, the results of the simulations and experiments are given and discussed in detail. The conclusion section summarizes the key outcomes of the study.

2 METHODS AND MATERIALS

The numerical simulations and experiments were conducted to study the aerodynamic characteristics of the NACA 4415 airfoil which had a chord length of 105 mm, and the corresponding Reynolds number was 85·10³. During the studies, the effect of the aspect ratio on the coefficients of lift and drag was investigated. The aspect ratio is the ratio of the airfoil span and the chord length. The investigated aspect ratios within the scope of this study were 3, 5, 7, and 9. The aspect ratio is defined as;

$$AR = \frac{b^2}{S} = \frac{b}{c}, \tag{1}$$

where AR, b, c, and S indicate the aspect ratio, span, chord length, and the planform area of the airfoil, respectively. The Reynolds number is expressed as;

$$Re = \frac{\rho v c}{\mu}, \tag{2}$$

where Re, ρ, v, μ indicate the Reynolds number, density of the air, free stream velocity, and the dynamic viscosity, respectively. The formulae used for the calculation of the lift and drag coefficients are given as;

$$C_L = \frac{2F_L}{\rho v^2 S}, \tag{3}$$

$$C_D = \frac{2F_D}{\rho v^2 S}, \tag{4}$$

where F_L is lift force and F_D is drag force. C_L and C_D are the coefficients of lift and drag, respectively.

2.1 Numerical Procedure

2.1.1 Model Definition

The numerical results of this study were obtained for a NACA 4415 airfoil profile. Boundary conditions had been set as velocity inlet, pressure outlet, and the wall along the airfoil and along the sides of the computational domain except for the right side. The symmetry was applied to the right side of the domain to decrease the number of elements created and accordingly the computational time.

2.1.2 Mesh Independence Study

Both hexahedral - tetrahedral and hexahedral - polyhedral meshes were created to observe the effect of meshes on the simulation time. Fig. 2 provides mesh details of the computational domain. The computational domain was divided into two parts to generate more successful mesh grids. The mesh quality in the near-field area
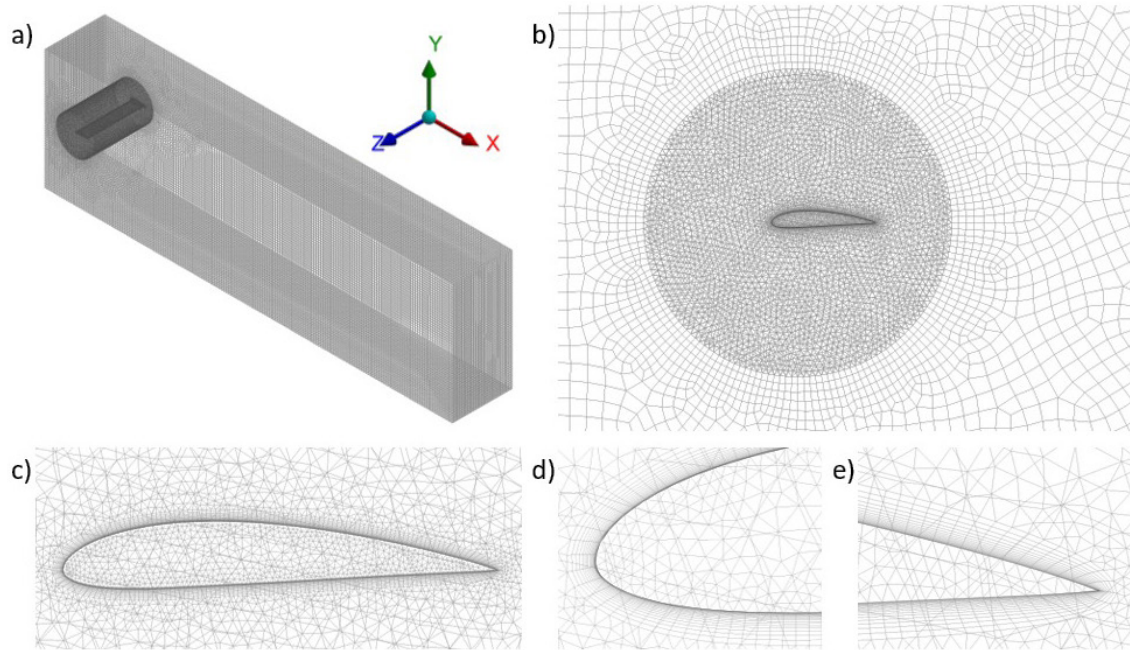
Fig. 2. Mesh details; a) computational domain; magnified mesh view around, b) the near-field, c) the airfoil; magnified view of the inflation layers around, d) the leading edge, and e) the trailing edge
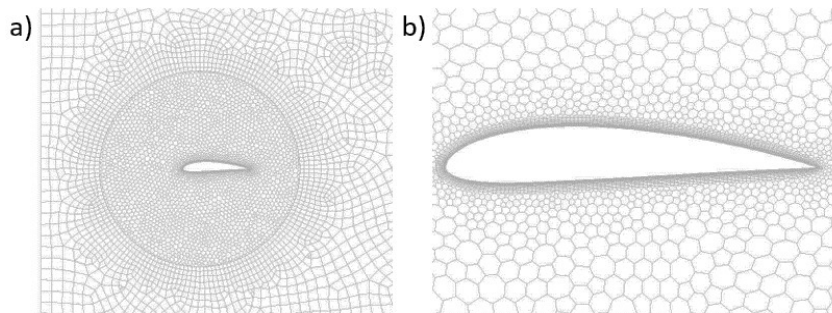
Fig. 3. a) Polyhedral mesh in the near-field area, and b) magnified view of the polyhedral mesh around the airfoil

around the airfoil was improved using the body sizing and face sizing method. The sizing option of the overall mesh was proximity and curvature. Inflation layer with 20 layers and a growth rate of 1.2 was employed along the airfoil wall to provide the y+ < 5 requirement. y+ values were around 1 for all analyses performed in this study. The mesh statistics show that the number of nodes was 1730042 and the orthogonal quality was 0.88.

The simulations were run using ANSYS® Fluent on a computer with Intel Core i7- 6700HQ, 2.6 GHz CPU and 16 GB RAM. To reduce the convergence time and complete the analysis in a shorter time, polyhedral meshes were used in the flow analysis. It means that converting the tetrahedral mesh to the polyhedral mesh affects the computational expense positively. Table 1 summarizes the relation between the simulation time and the applied meshes and Fig. 3 shows the polyhedral mesh details.

Table 1. The effect of tetrahedral and polyhedral meshes on convergence time at grid level = 4 at 0° AoA for AR = 9

	Hexahedral & Tetrahedral	Hexahedral & Polyhedral
Average time per iteration [s]	9.778	4.813
Total convergence time [s]	12799	2411

Table 2. Mesh independence study at 0° AoA for AR = 9

grid #	max face size [m]	max size [m]	body & face sizing [m]	# of nodes	orthogonal quality	y^+	C_L/C_D	average time per iteration [s]
1	3e-2	5e-2	1.5e-2	637048	0.83	1.05357	10.11	2.372
2	1.8e-2	2e-2	1e-2	1089297	0.86	1.05652	10.15	3.125
3	1.8e-2	2e-2	8e-3	1268383	0.87	1.05936	10.21	3.550
4	1.8e-2	2e-2	6e-3	1730042	0.88	1.05980	10.32	4.813
5	1.5e-2	1.8e-2	6e-3	2115060	0.89	1.06013	10.32	5.684
6	1.2e-2	1.5e-2	6e-3	2807537	0.90	1.06237	10.32	7.244

Table 2 presents the results of the mesh independence study. Mesh quality affects both computational accuracy and computational time. The optimum element number is the point where the results are accurate with the fewest elements. 4th grid was chosen for the simulation not to increase the number of nodes and the computational time. Fig. 4 shows the relation between the grid level and C_L/C_D.
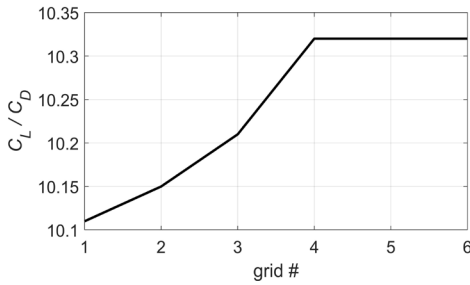
Fig. 4. Grid # and C_L/C_D relation

2.1.3 Simulation Setup

As a turbulence model, k–ω SST with a standard set of coefficients was selected. The SIMPLE scheme was used to handle the pressure-velocity coupling. Second-order upwind discretization scheme was applied for all RANS equations due to its balance of accuracy and computational efficiency. The residual convergence level of the simulations was 10^{-7}. The governing equations of the k–ω SST turbulence model are given by:

$$\frac{\partial(\rho k)}{\partial t} + \frac{\partial(\rho U_j k)}{\partial x_j} = P_k - C_\mu \rho k \omega + \frac{\partial}{\partial x_j}\left[\left(\mu + \frac{\mu_t}{\sigma_k}\right)\frac{\partial k}{\partial x_j}\right], \tag{5}$$

$$\frac{\partial(\rho \omega)}{\partial t} + \frac{\partial(\rho U_j \omega)}{\partial x_j} = C_{\omega 1}\frac{\omega}{k}P_k - C_{\omega 2}\rho\omega^2 + \rho\left(1 - F_1\right)CD$$
$$+ \frac{\partial}{\partial x_j}\left[\left(\mu + \frac{\mu_t}{\sigma_\omega}\right)\frac{\partial \omega}{\partial x_j}\right], \tag{6}$$

where k, ω, μ_t, σ_k, σ_ω, CD, F_1, $C_{\omega 1}$ and $C_{\omega 2}$ represent the turbulence kinetic energy, specific dissipation rate, turbulent viscosity, turbulent Prandtl numbers for k and ω, cross-diffusion term, blending function, and model coefficients, respectively. Simulation parameters are presented in Table 3.

Table 3. Simulation parameters

Turbulence model	k–ω SST with a standard set of coefficients
Solver	Pressure based SIMPLE scheme
Discretization	Second-order upwind scheme
Residual convergence level	10^{-7}

2.2 Experimental Setup

At the İzmir Kâtip Çelebi University, Turkey, a wind tunnel was employed to conduct experiments. The airfoil's mounting frame was constructed from 30 mm × 30 mm aluminum profiles, as depicted in Fig. 5. The wind tunnel features an open-square jet section with dimensions of 1000 mm × 1000 mm and has a maximum freestream velocity of 12 m/s. The three-component balance system provided structural support to the airfoil, which was attached via a shaft at its quarter chord, and had a protractor on it that allows to set the airfoil's attack angle. A series of force measurements were conducted using the three-component balance for the investigation of the airfoil's aerodynamic performance. Before the measurements, the

wind-off load was subtracted to calibrate the measurement system. The resulting force values were read from the display unit, and the force values were evaluated using the calibration table which was generated before the measurements.

NACA 4415 airfoil was modeled using a CAD program, and the airfoil model was fabricated by a three - dimensional (3D) printer using PLA material. The software's printing settings were configured with the following specifications: layer height at 0.2 mm, wall thickness at 1.5 mm, wall line count at 3, and infill density at 15 %. Also, a tri-hexagon infill pattern was used as an internal structure of the airfoil. Fig. 6 shows the 3D printed airfoil model.
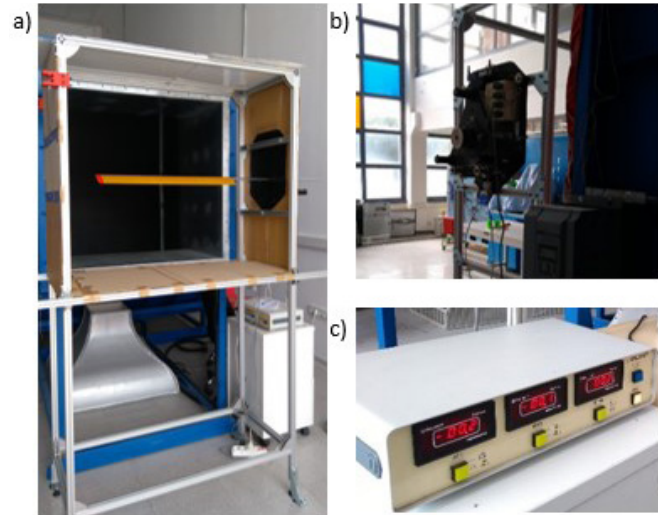
Fig. 5. Experimental setup; a) low-speed wind tunnel,
b) three-component balance, and c) display unit

3 RESULTS AND DISCUSSIONS

The numerical simulation results are utilized to support the interpretation of the experimental part of this study. To interpret the results, the velocity vectors and the vortices around the airfoil are investigated. To investigate the separation characteristics of the airfoil, the vector representation of the flow is given in Fig. 7. Red arrows in the figure show the separation points. As the aspect ratio and angle of attack increase, it can be seen that the separation points move towards the leading edge of the airfoil. For low aspect ratios flow remains largely attached to the airfoil at low angles of attack. However, separation is stronger for high aspect ratio airfoils compared to low aspect ratios. In other words, it has been observed numerically that stall occurs at smaller angles of attack as the aspect ratio increases. The performed experiments are compatible with the data obtained as a result of numerical analysis.

Flow rolls around the tip of the airfoil from bottom to top, and it is called tip vortex. Lambda2 vortex criterion is a detection method of the vortices from a 3D flow. The method is used to identify and analyze regions of rotational motion and they are visualized using ANSYS® Fluent. Fig. 8 depicts the iso-surface plots of the Lambda2 criterion and tip vortices can be seen at the tip of the airfoil for all AoA and the aspect ratios. It appears that the tip vortices do not change with increasing AoA. However, the spanwise vortices form through the airfoil, and they grow with the increasing AoA. At low AoA, the spanwise vortices are weaker and more evenly distributed across the span of the airfoil. As AoA increases, the strength of the spanwise vortices increases. At higher AoA, while vortex structures grow larger, the flow remains more organized for lower aspect ratio airfoils than higher AR airfoils.

Fig. 6. 3D printed airfoil model; a) top-view, and b) side-view
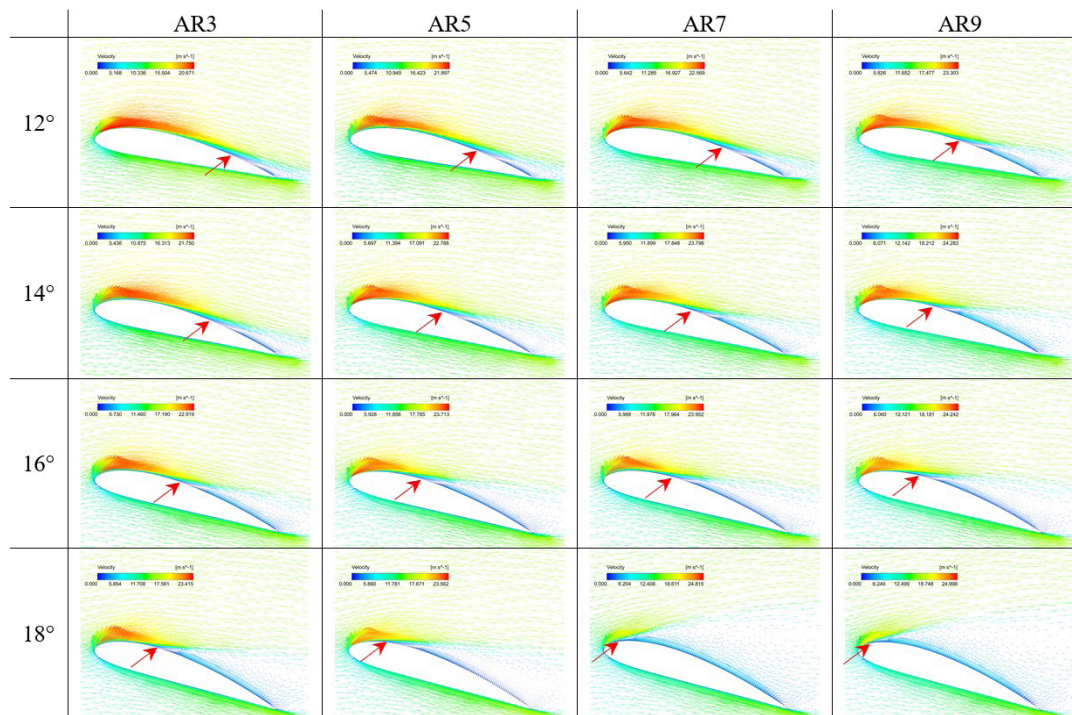
Fig. 7. Separation characteristics of airfoils with different aspect ratios at Re = 85·10³ (red arrows represent separation)
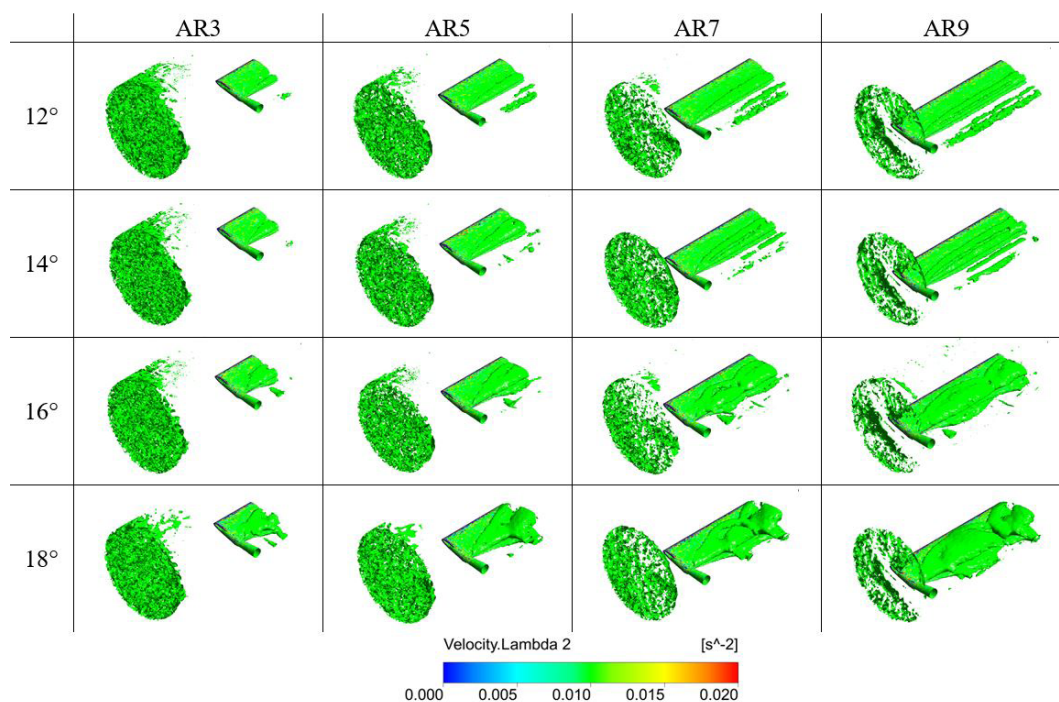
Fig. 8. Iso-surface plots of Lambda2 criterion

The aerodynamic coefficients' relation with the AoA is given in Fig. 9, and the stall angles have been examined in detail concerning AR and AoA relations. The results are obtained for the different aspect ratios of the airfoil, and the aspect ratio effect is observed on the NACA 4415 airfoil with chord length of 105 mm. The findings of the present study are consistent with the results of Miley [23], and

Ostowari and Naik [24] studies given in the introduction part. As compared to Ostowari and Naik [24] study, the presented experiments are conducted at a lower Reynolds number condition, and thus, the maximum lift coefficients are lower than their study as expected. Also, Miley [23] shows that when the Reynolds number is lower, the stall happens at lower angles of attack.

Firstly, the outcomes of the experiments are presented. The maximum lift coefficient for aspect ratio of 3 is 0.864 and the corresponding angle of attack is 18°. The maximum lift happens at 17° of angle of attack for aspect ratio of 5 and the value of the lift coefficient is 0.965. For aspect ratio 7, the maximum lift occurs at 15° of angle of attack and it is 1.068. The maximum lift coefficient is 1.164 for aspect ratio 9 and the corresponding angle of attack is 13°.

Secondly, the results of the numerical studies are shared. The maximum lift coefficient is 1 for the aspect ratio of 3 and it occurs at 18° of angle of attack. For aspect ratio 5, the maximum lift happens at 16° of angle of attack and the value of the lift coefficient is 1.05. The maximum lift coefficient for the aspect ratio of 7 is 1.09 and the maximum lift occurs at 15° of angle of attack. Aspect ratio of 9 has a maximum lift coefficient of 1.19 at 13° of angle of attack.

The maximum lift coefficient difference between the experimental and numerical results gets closer as the aspect ratio increases from 3 to 9. In airfoils with low aspect ratios, three-dimensional characteristics like flow separation and tip vortices are significant. Higher aspect ratios reduce these three-dimensional effects, resulting in more two-dimensional flow and improved agreement between numerical and experimental data. The percentage difference rates are 15.74 %, 8.81 %, 2.83 %, and 2.23 % for aspect ratios of 3, 5, 7, and 9, respectively. The results of the numerical studies and the experiments show similar tendencies. Although there are differences in the maximum lift values, stall angles are coherent. The results of the experimental and numerical studies are presented in Table 4.

Table 4. Comparative data of the experimental and the numerical studies

	max C_L (experimental)	max C_L (numerical)	% Difference	Corresponding AoA
AR3	0.864	1	15.74	18°
AR5	0.965	1.05	8.81	16° to 17°
AR7	1.068	1.09	2.83	15°
AR9	1.164	1.19	2.23	13°
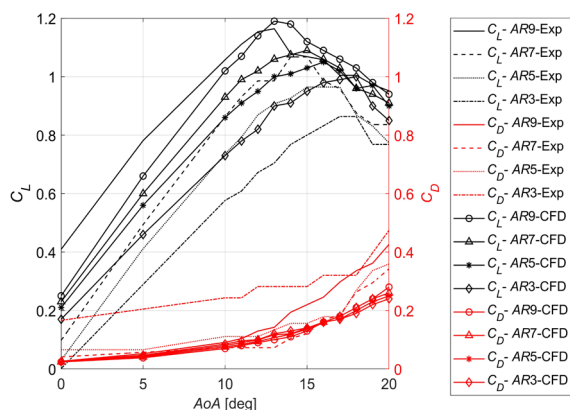
Fig. 9. Comparison of the experiment and CFD results

As the numerical and experimental results of the drag coefficients are compared, they are in harmony in certain AoAs except for the aspect ratio of 3. The experimental results are higher than the numerical result of aspect ratio of 3 for all angle of attacks. For aspect ratio 5, the difference between the experimental and numerical

results is observed after 17° of angle of attack and the situation is the same for the aspect ratio of 7. The difference begins at 13° of angle of attack for aspect ratio of 9. The numerical results of the drag coefficients are very close to each other and they are sorted from aspect ratio of 9 as the smallest and 3 as the highest and after 16° the sequence turns the opposite.

4 CONCLUSIONS

Experimental measurements and flow analysis were performed to observe the influence of the various aspect ratios on the aerodynamic characteristic of the NACA 4415 airfoil profile for low Reynolds number. A low-speed, open section wind tunnel was used during the experiments. Also, a three-component balance system was utilized to measure the forces on the airfoil for different angles of attack. The lift and drag coefficients were calculated using obtained forces. ANSYS® Fluent software was used for comparing the results of the 3D flow analysis with the findings of the experiments.

The results of the experiments and the numerical studies show that with the increasing *AR*, the lift coefficients increase. Furthermore, the angles of attack in which the maximum lift is obtained, decrease with the increasing AR of the airfoil. Namely, the stall angle which is a critical parameter in airfoil design for aerodynamic systems decreases. During the flow analysis with the increasing AR, the drag coefficients decrease until AoA of 16°, while the drag coefficients increase with the increasing *AR* after this AoA. In conclusion, there is compatibility between the experimental and the numerical results in terms of the aerodynamic coefficients of the airfoil.

Further studies are planned to examine the effect of aspect ratio on airfoils at higher angles of attack and low Reynolds numbers.

REFERENCES

[1] Mohammed, A., Lemu, H.G., Sirahbizu, B. Determining optimum rotary blade design for wind-powered water-pumping systems for local selected sites. *Strojn vestn-J Mech E* 67 214-22 (2021) **DOI:10.5545/sv-jme.2021.7104**

[2] Ganesan, T., Jayarajan, N. Aerodynamic analysis of mathematically modelled propeller for small UAV using CFD in different temperature conditions. *Strojn vestn-J Mech E* 69 444-454 (2023) **DOI:10.5545/sv-jme.2023.601**

[3] Kılavuz, F., Kiral, B.G. Design optimization of mechanical valves in dishwashers based on the minimization of pressure losses. *Strojn vestn-J Mech E* 70194-208 (2024) **DOI:10.5545/sv-jme.2023.768**

[4] Winslow, J., Otsuka, H., Govindarajan, B., Chopra, I. Basic understanding of airfoil characteristics at low reynolds numbers (104-105). J Aircraft 55 1050-1061 (2018) **DOI:10.2514/1.C034415**

[5] Akbıyık, H., Yavuz, H., Akansu, Y.E. A study on the plasma actuator electrode geometry configurations for improvement of the aerodynamic performance of an airfoil. Strojn vestn-J Mech E 64 719-725 (2018) **DOI:10.5545/sv-jme.2017.5041**

[6] Bartl, J., Sagmo, K.F., Bracchi, T., Sætran, L. Performance of the NREL S826 airfoil at low to moderate Reynolds numbers-A reference experiment for CFD models. *Eur J Mech B-Fluid* 75 180-192 (2019) **DOI:10.1016/j.euromechflu.2018.10.002**

[7] Traub, L.W., Coffman, C. Efficient low-reynolds-number airfoils. *J Aircraft* 56, 1987-2003 (2019) **DOI:10.2514/1.C035515**

[8] Xia, T., Dong, H., Yang, L., Liu, S., Jin, Z. Investigation on flow structure and aerodynamic characteristics over an airfoil at low Reynolds number-A review. *AIP Adv* 11 (2021) **DOI:10.1063/5.0044717**

[9] Murayama, Y., Nakata, T., Liu, H. Flexible flaps inspired by avian feathers can enhance aerodynamic robustness in low Reynolds number airfoils. *Front Bioeng Biotech* 9 612182 (2021) **DOI:10.3389/fbioe.2021.612182**

[10] Ayaz Ümütlü, H.C., Kıral, Z., Karadeniz, Z.H. A Preliminary experimental study on the effect of Reynolds number on the lift and drag of a NACA-4415 airfoil. *6th International Students Science Congress Proceedings Book*. 1-5 (2022) **DOI:10.52460/issc.2022.047**

[11] Stutz, C., Hrynuk, J., Bohl, D. Investigation of static wings interacting with vertical gusts of indefinite length at low Reynolds numbers. *Exp Fluids* 63 82 (2022) **DOI:10.1007/s00348-022-03432-7**

[12] Somashekar, V., Immanuel Selwynraj, A. Aerodynamic study of low Reynolds number airfoil and mini-unmanned aerial vehicle in simulated rain environment. *Aircr Eng Aerosp Tec* 94 1748-1758 (2022) **DOI:10.1108/AEAT-12-2021-0379**

[13] Ananda, G.K., Sukumar, P.P., Selig, M.S. Measured aerodynamic characteristics of wings at low Reynolds numbers. *Aerosp Sci Technol* 42 392-406 (2015) **DOI:10.1016/j.ast.2014.11.016**

[14] Lee, Y.J., Lua, K.B., Lim, T.T. Aspect ratio effects on revolving wings with Rossby number consideration. *Bioinspir Biomim* 11 56013 (2016) **DOI:10.1088/1748-3190/11/5/056013**

[15] Awasthi, M., Moreau, D.J., Doolan, C.J. Flow structure of a low aspect ratio wall-mounted airfoil operating in a low Reynolds number flow. *Exp Therm Fluid Sci* 99 94-116 (2018) **DOI:10.1016/j.expthermflusci.2018.07.019**

[16] Zanforlin, S., Deluca, S. Effects of the Reynolds number and the tip losses on the optimal aspect ratio of straight-bladed vertical axis wind turbines. *Energy* 148 179-195 (2018) **DOI:10.1016/j.energy.2018.01.132**

[17] Lee, S.H., Han, Y.O. Experimental investigation of high-angle-of-attack aerodynamics of low-aspect-ratio rectangular wings configured with NACA0012 airfoil section. *Internat J Aeronaut Space* 21 303-314 (2020) **DOI:10.1007/s42405-019-00215-z**

[18] Ayaz Ümütlü, H.C., Kiral, Z., Karadeniz, Z.H. Experimental investigation of NACA 4415 airfoil using vibration data for stall detection. *Aircr Eng Aerosp Tec* 95 1551-1559 (2023) **DOI:10.1108/AEAT-03-2023-0077**

[19] Asr, M.T., Nezhad, E.Z., Mustapha, F., Wiriadidjaja, S. Study on start-up characteristics of H-Darrieus vertical axis wind turbines comprising NACA 4-digit series blade airfoils. *Energy* 112 528-537 (2016) **DOI:10.1016/j.energy.2016.06.059**

[20] Parker, C.M., Araya, D.B., Leftwich, M.C. Effect of chord-to-diameter ratio on vertical-axis wind turbine wake development. *Exp Fluids* 58 186 (2017) **DOI:10.1007/s00348-017-2451-6**

[21] Zhong, J., Li, J., Guo, P., Wang, Y. Dynamic stall control on a vertical axis wind turbine aerofoil using leading-edge rod. *Energy* 174 246-260 (2019) **DOI:10.1016/j.energy.2019.02.176**

[22] Song, C., Wu, G., Zhu, W., Zhang, X. Study on aerodynamic characteristics of darrieus vertical axis wind turbines with different airfoil maximum thicknesses through computational fluid dynamics. *Arab J Sci Eng* 45 689-698 (2020) **DOI:10.1007/s13369-019-04127-8**

[23] Miley, S.J. *Catalog of low-Reynolds-number airfoil data for wind-turbine applications* (1982) **DOI:10.2172/5044823**

[24] Ostowari, C., Naik, D. Post stall studies of untwisted varying aspect ratio blades with an NACA 4415 airfoil section-Part I. *Wind Eng* 8 176-194 (1984)

Author contribution *Ayaz Ümütlü HC, Kıral Z, and Karadeniz ZH conceived the experiment. Ayaz Ümütlü HC operated the experiment and analyzed the data. The first draft of the manuscript was written by Ayaz Ümütlü HC. Kıral Z and Karadeniz ZH reviewed and edited the manuscript, and provided guidance.*

Numerična in eksperimentalna raziskava vpliva vitkosti krila na aerodinamične lastnosti profila NACA 4415 pri nizkem Reynoldsovem številu

Povzetek *V tej študiji je raziskan vpliv vitkosti krila na aerodinamične koeficiente profila krila NACA 4415. S simulacijami računalniške dinamike tekočin (CFD) in eksperimenti so obravnavane štiri različne vrednosti vitkosti kril, in sicer 3, 5, 7 in 9. CFD analize so izvedene s tridimenzionalno (3D) računsko domeno, za izračun turbulence pa se uporablja model k-ω za prenos strižne napetosti (SST). Meritve aerodinamičnih sil so bile opravljene v vetrovniku z odprtim tokom z uporabo tri-komponentnega merilnika sil. CFD analize in eksperimentalne meritve so bile izvedene pri naklonskih kotih od 0° do 25° in Reynoldsovem številu 85·10³. Rezultati kažejo, da se s povečevanjem vitkosti krila ločilne točke pomikajo proti sprednjemu robu krila in da se kritični vpadni kot zmanjšuje. Poleg tega je opaziti, da se koeficient vzgona povečuje z naraščajočo vitkostjo krila. Dobljeni rezultati kažejo, da obstaja skladnost med eksperimentalnimi meritvami in rezultati CFD analiz.*

Ključne besede *aerodinamični profil, vetrovnik, vitkost krila, aerodinamični koeficienti, tri-komponentni merilnik sil, nizko Reynoldsovo število*